Clinical Cancer Research

Cancer Therapy: Preclinical

Dietary Curcumin Attenuates Glioma Growth in a Syngeneic Mouse Model by Inhibition of the JAK1,2/STAT3 Signaling Pathway

Jakob Weissenberger[1], Maike Priester[1], Christian Bernreuther[2], Stefanie Rakel[1], Markus Glatzel[2], Volker Seifert[3], and Donat Kögel[1]

Abstract

Purpose: Glioblastomas are the most common and most deadly primary brain tumors. Here, we evaluated the chemotherapeutic effect of the natural polyphenol curcumin on glioma cells *in vitro* and *in vivo* using an immunocompetent orthotopic mouse model.

Experimental Design: Curcumin's effects on proliferation, cell cycle, migration, invasion, JAK/STAT3 signaling, STAT3 target gene expression, and STAT3C rescue experiments were determined in murine glioma cell lines *in vitro*. Therapeutic effects of curcumin *in vivo* were evaluated in tumor-bearing mice fed a Western-type diet fortified with curcumin (0.05%, w/w) and in control animals. Tumor growth patterns and survival were evaluated by immunohistochemistry, morphometric analyses, and Kaplan–Meier plots.

Results: *In vitro*, curcumin inhibited JAK1,2/STAT3 tyrosine-phosphorylation in a dose-dependent fashion in murine glioma cell lines. Real-time RT-PCR revealed that curcumin downregulated transcription of the STAT3 target genes c-Myc, MMP-9, Snail, and Twist, and of the proliferation marker Ki67. Curcumin dose-dependently suppressed cell proliferation by inducing a G2/M phase arrest. In wound healing and Matrigel invasion assays, curcumin treatment resulted in a dose-dependent attenuation of the glioma cells' migratory and invasive behavior, which could be rescued by constitutively active STAT3C. *In vivo*, curcumin intake reduced the growth and midline crossing of intracranially implanted tumors and proliferation of tumor cells ensuing in significant long-term survival compared with control diet.

Conclusion: This preclinical study shows that curcumin is capable of suppressing malignant glioma growth *in vitro* and *in vivo*. Our data suggest that the pharmacologically safe agent curcumin holds promise for clinical application in glioma therapy. *Clin Cancer Res; 16(23); 5781–95. ©2010 AACR.*

Despite major advances in the diagnosis and treatment of cancer in recent years, glioblastoma multiforme (GBM) is still rarely curable and most patients diagnosed with GBM die within a year (1). Because malignant gliomas inherently show poor response to standard treatment protocols that routinely consist of surgical debulking followed by either implantation of Gliadel or oral temozolomide combined with radiation therapy (2, 3), the development and testing of more effective chemotherapeutic agents is direly needed.

Agents that are safe and can be administered as dietary supplements appear to be most feasible for therapy. The polyphenol curcumin, naturally occurring in the spice plant turmeric (*Curcuma longa*), exhibits minimal toxicity while acting through pleiotropic mechanisms including NF-κB suppression, COX-2 downregulation, and Wnt and Notch pathway downregulation (4). Treatment of human GBM cells with curcumin in cell cultures or after xenografting in immunocompromised mice resulted in growth suppression, cell cycle arrest, inhibition of multiple matrix-metalloproteinases, and induction of apoptosis or autophagy (5–8). These anticancer effects were attributed to curcumin's interference with the NF-κB, ERK, AKT, or mTOR signaling pathways. Despite the fact that STAT3 is constitutively activated in the majority of malignant gliomas (described in the following text), no study has addressed the relevance of the JAK/STAT3 signaling pathway in this context so far.

The etiology of malignant gliomas is still not fully resolved; however, accumulating evidence points to a multistep process involving accumulation of aberrations in signaling pathways influencing cell proliferation and survival such as AKT, ERK, mTOR, and JAK/STAT3 (9).

Authors' Affiliations: [1]Experimental Neurosurgery, Center of Neurology and Neurosurgery, Goethe University Hospital, Frankfurt, Germany; [2]Institute of Neuropathology, University Medical Center Hamburg-Eppendorf, Hamburg, Germany; and [3]Department of Neurosurgery, Goethe University Hospital, Frankfurt, Germany

Note: Supplementary data for this article are available at Clinical cancer Research Online (http://clincancerres.aacrjournals.org/).

J. Weissenberger, M. Priester, and C. Bernreuther contributed equally to the work.

Corresponding Author: Jakob Weissenberger, Experimental Neurosurgery, Center of Neurology and Neurosurgery, Goethe University Hospital, Neuroscience Center, Heinrich-Hoffmann-Straße. 7, D-60592 Frankfurt, Germany. Phone: 069 6301 84051; Fax: 069 6301 5575. E-mail: j.weissenberger@med.uni-frankfurt.de

doi: 10.1158/1078-0432.CCR-10-0446

Translational Relevance

Gliomas are a heterogeneous group of tumors among which aberrant activation of the JAK/STAT3 signaling pathway has been associated with aggressiveness. The identification of inhibitors targeting this pathway is therefore of substantial interest to devise more efficient therapies. Here, we used a novel immunocompetent mouse model to evaluate the antiglioma effects of the natural polyphenol curcumin. Low doses of curcumin potently inhibited JAK/STAT3 activity, glioma cell proliferation, migration, and invasion; the latter being a major cause for current treatment failure. Tumor-bearing mice fed a curcumin-supplemented Western-type diet experienced increased long-term survival suggesting that the chemotherapeutic agent can prevent or limit tumor growth and may increase the sensitivity of malignant glioma cells to current treatment regimens. Because Curcumin is safe, it could be easily translated into the clinic to improve the life expectancy of patients with malignant glioma.

STAT3 is a member of the STAT family of transcription factors that are tightly regulated under physiologic conditions and become transiently activated in response to cytokine and growth factor receptor as well as nonreceptor kinase stimulation, all of which were frequently found to be aberrantly active in glial tumors (10). On receptor stimulation, latent STAT3 proteins in the cytoplasm become phosphorylated by receptor-associated kinases, and then form dimers that translocate to the nucleus, where they act as transcription factors. Interestingly, STAT3 activity is required for self-renewal of embryonic stem cells and for proliferation and maintenance of multipotency of glioblastoma stem cells (11). Although STAT3 deficiency is embryonically lethal (E7.0), STAT3 appears to be dispensable in most adult tissues (12). However, selective loss of STAT3 in keratinocytes resulted in impaired wound healing, and skin-specific ablation of STAT3 lead to psoriasis in transgenic mice (13, 14). On the other hand, persistent activation of STAT3 was shown to be a strong promoter of oncogenesis (15) by inciting cell proliferation, conferring resistance to apoptosis, inducing angiogenesis, and mediating immune evasion (16). The fact that transformed but not normal cells depend on STAT3 (17) makes it an attractive target for therapeutic intervention.

We have previously shown that constitutive STAT3 activation occurs in human and murine gliomas that it correlates with malignancy, and that ablation of the cytokine IL-6, which signals through the JAK/STAT3 pathway, prevents tumor development in otherwise tumor-prone mice (18). Interference with IL-6 signaling also resulted in suppression of glioma stem cell survival and tumor growth of human glioma xenografts in nude mice (19). Curcumin was shown to inhibit constitutive and IL-6–induced STAT3 activation in human multiple myeloma cells (20), and interference with the STAT3 signaling pathway by siRNA-induced apoptosis in cultured astrocytoma cells (21). Furthermore, the small-molecule STAT3 inhibitor, WP1066, restrained subcutaneous tumor growth of glioma cells in nude mice (22).

To determine whether the natural polyphenol curcumin is able to avert brain tumor formation in an authentic microenvironment, we examined the effects of the compound in an orthotopic and immunocompetent mouse model of glioma that faithfully mirrors the hallmarks of human gliomas (23). We show that curcumin antagonizes the glioma-typical growth characteristics of the mouse cell lines Tu-2449, Tu-9648, and Tu-251 and provide evidence that these effects are mediated through inhibition of the JAK1,2/STAT3 signaling pathway.

Materials and Methods

Antibodies and reagents

Rabbit polyclonal phospho-JAK1 (Tyr1022/1023) and phospho-JAK2 (Tyr107/1008) antibodies were both purchased from Calbiochem through Merck. Rabbit polyclonal phospho-STAT3 (Tyr705) antibody was purchased from Cell Signaling Technology and mouse monoclonal STAT3 (C-20) antibody was obtained from Santa Cruz. For *in vitro* studies, more than 94% pure curcumin (LKT laboratories) was prepared as a 2.952 mmol/L stock solution in dimethyl sulfoxide (DMSO). For *in vivo* studies, the same reagent was added to a Western-type diet (Altromin; enriched with 21% milk fat and 0.15% cholesterol, w/w). Curcumin (0.05%, w/w) was uniformly incorporated into the mouse chow to ensure even curcumin intake. All control and experimental diets were pelleted, vacuum packed, and stored at 4°C in the dark.

Animals

Female 10-week-old C6B3F1 mice (Harlan-Winkelmann) were kept under controlled conditions of light (12 hours light–dark cycles) and temperature (20°C–25°C), and fed a control diet (Western-type) or an experimental diet (Western-type plus curcumin) *ad libitum* and free access to water. Each mouse consumed approximately 4 g mouse chow per day. There was no significant difference in water or food consumption between groups.

Cell lines

Tu-2449, Tu-9648, and Tu-251 glioma cell lines, derived from spontaneous mouse brain tumors (24), were maintained in high glucose (4.5 g/L) Dulbecco's modied Eagle's medium (Gibco) supplemented with 10% fetal calf serum (FCS), 100 U/mL penicillin, and 100 mg/mL streptomycin in a humidified 5% CO_2 atmosphere at 37°C. Cells were split twice a week. All experiments were performed with cells in the logarithmic growth phase.

Plasmid transfection

A mammalian expression vector harboring a constitutive active STAT3 (STAT3C) was used for rescue experiments

(25). Transient transfection of murine glioma cells using FuGENE HD Transfection Reagent (Roche) was performed at 60% cell confluence with 1 μg of STAT3C in 6-well plates. Cells were kept for another 24 hours before scratching or seeding in Boyden chambers. For control of rescue experiments, cells were transfected with 1 μg of parent vector pYN3218.

3-(4,5-Dimethylthiazol-2-yl)-2,5-diphenylterazolium bromide assay

Viability was assessed with the 3-(4,5-dimethylthiazol-2-yl)-2,5-diphenylterazolium bromide (MTT) assay as described previously (26). Briefly, 96-well microculture plates (Greiner Bio-One) contained a total volume of 100 μL cell suspension (2×10^5 per mL) in complete medium. All drug concentrations and untreated controls were set up 3-fold. After incubation for 24, 48, and 72 hours, 20 μL of MTT solution (Sigma-Aldrich) was added for 3 hours. MTT is reduced to colored formazan by living cells but not by dead cells. The formazan crystals were dissolved with 100 μL of 0.04 N of HCl-isopropanol. Absorbance of the wells was determined with a microculture plate reader (Tecan) at 570 nm test wavelength and 690 nm reference wavelength.

Cell cycle analysis

Cells attached to the culture dish were trypsinized and collected together with the cells floating in the medium. These cells were washed in PBS and fixed in 70% (v/v) ethanol. Fixed cells were washed once again with PBS, followed by incubation in PBS containing 50 μg/mL propidium iodide (Sigma-Aldrich) and 20 μg/mL RNase A (Sigma-Aldrich) for 30 minutes at room temperature in the dark. The DNA content was then analyzed using a Becton Dickinson FACScan with 100 to 150 events per second. BD FACSDiva software was used to assess cell cycle distribution.

Caspase cleavage assay

Cells used for *in vitro* effector caspase activity assays were lysed, followed by the addition of buffer containing DEVD-7-amino-4-methylcoumarin (AMC) as described previously (27). Briefly, lysates were incubated for 2 hours at 37°C in the dark and the generation of the fluorescent AMC cleavage product was measured at 380 nm excitation and 465 nm emission, using a fluorescence plate reader.

Migration (scratch) assay

Tu-2449, Tu-9648, and Tu-251 cells were plated at 1.5×10^5 per well in an uncoated 6-well plate (Greiner Bio-One). When the cells had reached subconfluency, they were treated with curcumin for 24 hours, and then mitomycin C (10 μg/mL) was added to the medium for 2 hours and a scratch was made using a sterile pipette tip. Photographs of the scratched area were taken at 0 hour and after 16 hours using a Eclipse TE2000-S microscope (Nikon), and the number of cells that had migrated over the margin of the scratch was counted. The scratch was captured in 5 different photographs and the numbers of migrated cells were averaged. Experiments were repeated 3 times.

Invasion (Matrigel) chamber assay

Tu-2449, Tu-9648, and Tu-251 cells (2.5×10^4) were seeded on a cell culture transwell insert coated with extracellular matrix (ECM); 8 μm pore size, 24-well format (Becton Dickinson) in 2% medium with different curcumin concentrations, and complete medium (10% FCS) was added to the lower chamber. To determine the amount of invasion, cells were incubated for 24 hours and then removed from the upper chamber using a cotton swab. The invaded cells on the downside of the insert were fixed with methanol (2 minutes). Once fixed, the cells were stained with crystal violet for 2 minutes and rinsed with PBS. The downsides of the membrane were then photographed to compare the number of invaded cells per insert. The transmigrated cells were counted using a Nikon Eclipse TE2000-S microscope (Nikon). For each experiment, 10 random high-power fields (HPF) were counted.

RNA isolation and first-strand synthesis

Total RNA was extracted from Tu-2449 and Tu-9648 cells using the RNAeasy Plus Mini Kit (Qiagen). RNA quality and concentration was measured using the Biophotometer (Eppendorf). A total of 1 μg of RNA, 200 ng of random primer, 250 ng oligo (dT) primer, 10 μmol dNTPs, and 200 units of Supercript III M-MLV Reverse Transcriptase (Invitrogen) were used in 1 reverse transcription reaction . The reverse transcription reaction was run at 50°C for 1 hour and then inactivated at 70°C for 15 minutes.

Quantitative real-time PCR

cDNA (50 ng) were used to perform a TaqMan Gene Expression Assay in a final volume of 20 μL. The expression analysis was carried out in an ABI PRISM 5700 Sequence Detection System (Applied Biosystems) and 96-well MicroPlates (Applied Biosystems). For all reactions, the TaqMan Universal PCR Master Mix, No AmpErase UNG (Applied Biosystems) was used. Primers and probes for TaqMan PCR were obtained from Applied Biosystems' predesigned TaqMan Gene Assays (c-Myc, Mm00487804_m1; Bcl-2, Mm0047763_m1; BcL-xL, Mm00437783_M1; MMP-9, Mm00600163_m1; Snail, Mm01249564_g1; Twist, Mm00442036_m1; Ki67, Mm01278617_m1). Applied PCR conditions were 50°C for 2 minutes and 95°C for 10 minutes followed by 40 cycles at 95°C for 15 seconds and at 60°C for 40 seconds. All assays were run in triplicates. Analysis of relative gene expression data was performed employing the $2^{-\Delta\Delta C(t)}$ method with the hypoxanthine guanine phosphoribosyl transferase 1 (Hprt1) gene (Mm00446966_m1) as endogenous control/reference (28).

Western blot analysis

Treated and untreated Tu-2449, Tu-9648, and Tu-251 cells were harvested by trypsinization, washed with ice-cold

PBS, and lysed in a buffer containing 137 mmol/L Tris-HCl (pH 6.8), 4% SDS, 20% glycerol, protease inhibitor cocktail (Pierce) and phosphatase inhibitor cocktail (Pierce). A total of 50 μg of total protein, quantified with a BCA protein assay (Pierce), were separated through 10% SDS-PAGE and transferred to Protran (0.45 μm) nitrocellulose membranes (Schleicher & Schuell). The membranes were blocked with a 5% milk–TBST solution (0.05% Tween-20/TBS) and subsequently incubated in 3% milk–TBST (0.05% Tween-20/PBS) with the phospho-JAK1 (Tyr1022/1023) and phospho-JAK2 (Tyr107/1008), or phospho-STAT3 (Tyr705) antibody diluted at 1:1,000 overnight at 4°C, or with the STAT3α (C-20) antibody at a dilution of 1:1,000 for 2 hours at room temperature. After incubation with IRDye secondary antibody (LI-COR Bioscience) a dilution of 1:20000 for 2 hours, the bands were visualized with a LI-COR Odyssey reader (LI-COR Bioscience).

DNA-binding ELISA for active STAT3

Whole cell extracts of transiently transfected murine glioma cells were assayed in 96-well plate format, in which the activated STAT3 transcription factor binds at its consensus binding site on immobilized double-stranded oligonucleotides and is quantified colometrically after addition of STAT3 antibody following the recommendations of the vendor (Transfactor Kit, Clontech-Takara Bio Europe).

Mouse brain tumor model

Tu-2449 and Tu-9648 cells (1×10^5 in 1 μL) were implanted in the striatum (coordinates: 2.5 mm from the dura, 1.5 mm posterior, 2 mm lateral to the bregma) of 10-week-old C6B3F1 mice and fed a control or curcumin-supplemented diet. Tumor implantation was performed as previously described (23). Briefly, glioma cell suspensions were injected stereotaxically through a drilled bur hole with a 5 μL Hamilton syringe (#75N) into the left putamen. A small cavity was created by moving down the needle 0.5 mm deeper than the indicated depth before the cells were being injected carefully over a period of 30 seconds. The needle was then held in place for further 30 seconds before being withdrawn slowly. Mice were monitored daily for symptoms of tumor development. After 65 or 80 weeks, respectively, all mice were subjected to histopathologic examination. All animal procedures were carried out in accordance to the guidelines for the care and use of laboratory animals and were approved by the administrative court of the state of Hessia.

Analysis of mouse brains

For histologic analysis, brains were removed, fixed in zinc formalin solution (Thermo Shandon) for at least 48 hours, and then embedded in paraffin followed by routine hematoxylin and eosin (H&E) staining on 5-μm thick coronal sections using routine protocols. Analysis was done at the level of the largest cross-sectional area of the tumor. All procedures were carried out at room temperature. All slides were counterstained with alum–hematoxylin. Blocking of endogenous peroxidase activity was performed with 0.3% H_2O_2 for 15 minutes. The slides were treated in a microwave oven (750 W) for 15 minutes in 10 mmol/L citrate buffer (pH 6.0) for demascation of the antigen. Then rabbit polyclonal antibodies against Ki67 (ab15580, 1:100, Abcam), rabbit polyclonal antibodies against phosphorylated (Y705) STAT3 (ab30646, 1:100, Abcam), or mouse monoclonal antibodies against glial fibrillary acidic protein (GFAP, M0761, 1:100; Dako) in blocking buffer [5% goat serum/TBS (pH 7.6)/0.1% Triton X-100 in antibody diluent solution (Zytomed)], were applied overnight. Histofine immunoperoxidase polymer, anti-rabbit or Histofine mouse stain kit (both from Nichirei Biosciences Inc.) was applied after washing with TBS. The peroxidase reaction was detected using diaminobenzidine (Sigma-Aldrich) as chromogen. Morphometric analysis was performed in a blinded manner as described previously (29). Briefly, largest area occupied by the brain tumor (μm^2) was estimated in serial sections. The number of mitoses per 0.19 mm^2 HPF and the percentage of Ki-67–positive nuclei of all nuclei in 0.19 mm^2 were determined in at least 6 HPFs in each animal. For the analysis of necrosis, the following scoring system was used for H&E-stained sections (only tumor was assessed): 0 = no necrosis, 1 = solitary necroses, 2 = less than 50% of tumor area occupied by necroses, 3 = more than 50% of tumor area occupied by necroses; perforation of the brain surface (0, no; 1, yes); crossing of the midline (0, no; 1, yes); tumor cells migrating away from the tumor graft (0, none; 1, single cells; 2, <20 cells; 3, >20 cells). For the analysis of active STAT3, absolute numbers of tumor cells showing nuclear staining with antibodies against tyrosine-phosphorylated STAT3 (pY-STAT3) identified by counterstaining with alum–hematoxylin were determined in 0.19 mm^2 HPFs.

Statistical analysis

Histopathology and histomorphometry was performed in a blinded fashion. The survival curves were analyzed using the log-rank test employing the Prism GraphPad software (version 4.03, GraphPad Software Inc.). *In vitro* and *in vivo* tumor growth rates were determined by nonlinear regression analysis using Prism GraphPad software. NCSS statistical and power analysis software was used for statistical analysis of tumor size, *in vitro* cell growth. MTT, Scratch, Boyden-chamber assay, and RT-PCR data were analyzed by Student's *t* test or ANOVA. Differences between groups were considered significant at $P < 0.05$. All data are expressed as mean ± SEM.

Results

Curcumin prevents STAT3 activity by downregulating JAK1,2 activity

We have reported earlier that Tu-2449 and Tu-9648 cells persistently express active STAT3 (18, 23). Because STAT3 gets tyrosine-phosphorylated by upstream Janus kinases (JAKs) bound to the cytoplasmic tails of cytokine receptors

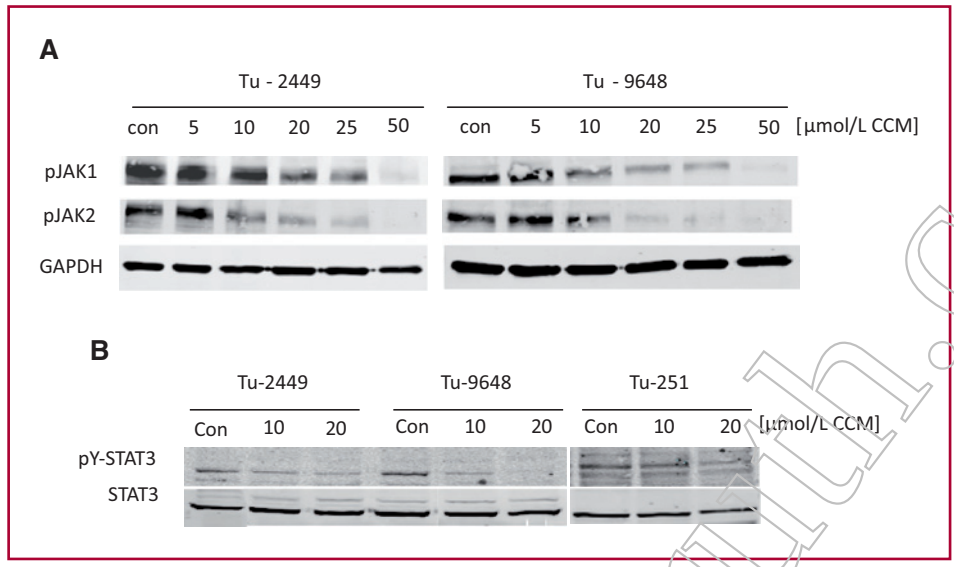

Fig. 1. A, curcumin prevents STAT3 activity by downregulation of JAK1,2 signaling in murine glioma cells. Tu-2449 and Tu-9648 cells were plated and grown for 24 hours and then treated with the solvent DMSO (Con) or indicated escalating doses of curcumin (CCM) dissolved in DMSO for 24 hours before harvesting. Cell lysates were analyzed by Western blotting for active JAK1,2 using specific antibodies to phospho-JAK1 (Tyr1022/1023) and phospho-JAK2 (Tyr107/1008). B, for analysis of the JAK substrate STAT3 the Tu-2449, Tu-9648, and Tu-251, glioma cells were treated similarly with solvent (Con) or 10 μmol/L, and 20 μmol/L curcumin (CCM), and immunoblotted for STAT3 activity using a specific antibody to phospho-STAT3 (pY-STAT3). Total STAT3 was also determined by stripping the membrane and using a pan-STAT3 antibody (STAT3α).

(30), we investigated whether curcumin might influence the JAK/STAT3 pathway and whether blockade of this pathway may account for the antiglioma activity of curcumin. Western blot analysis with phospho-specific antibodies to JAK1,2 performed on lysates of Tu-2449 and Tu-9648 cells cultured *in vitro* revealed that curcumin treatment dose-dependently downregulated the active tyrosine-phosphorylated forms of JAK1 and JAK2 (Fig. 1A). Likewise, the downstream JAK substrate STAT3 was inactivated in curcumin-exposed Tu-2449, Tu-9648, and Tu-251 cells. Curcumin inhibited the constitutive STAT3 activity in all 3 murine glioma cell lines in a dose-dependent fashion (Fig. 1B). STAT3 inhibition occurred already after 2 hours (data not shown) with complete abrogation in Tu-9648 cells after 24 hours incubation with the highest dose (20 μmol/L). Curcumin treatment did not change overall STAT3 protein expression.

Curcumin modulates expression of STAT3-dependent tumor-associated genes

To assess whether curcumin treatment of Tu-2449 and Tu-9648 cells elicits specific effects on STAT3-regulated genes both cell lines were treated with 10 μmol/L and 20 μmol/L curcumin for 24 hours and subsequently analyzed for mRNA expression of STAT3 target genes playing established roles in tumor growth, survival, migration, and invasion (Fig. 2). Most of the genes showed a dose-dependent response to the curcumin treatment, except for Bcl-xL and Bcl-2. When the highest dose (20 μmol/L) was employed, the cell cycle regulator c-Myc was markedly reduced in curcumin-treated cell lines (Tu-2449, 40%; Tu-9648, 60%) as was the diagnostic proliferation marker Ki67 (Tu-2449, 55%; Tu-9648, 40%) when compared with cells treated with the solvent DMSO as a control. The antiapoptotic gene Bcl-2 was only moderately affected in 1 cell line (Tu-2449), whereas expression of Bcl-xL was unchanged, which is keeping with the finding that curcumin did not induce caspase-dependent apoptosis in all cell lines tested (discussed in the following text). However, the invasion-relevant enzyme MMP-9 was dramatically downregulated by curcumin (Tu-2449, >80%; Tu-9648, 40%). In addition, the transcription factors Snail and Twist, which are associated with epithelial-mesenchymal transition, invasion, and metastasis, were reduced after curcumin treatment (Tu-2449, 55%; Tu-9648, 40%).

Curcumin slows proliferation of murine glioma cells

The above experiments showed that curcumin is a potent inhibitor of JAK1,2/STAT3 signaling and of STAT3-regulated tumor-promoting genes in Tu-2449 and Tu-9648 glioma cells. To examine the consequences of JAK1,2/STAT3 signaling inhibition on cell proliferation, we performed MTT assays to evaluate the potential inhibitory effect of curcumin on cell growth in 3 murine glioma cell lines Tu-2449, Tu-9648, and Tu-251 (Fig. 3A). Cells were exposed to escalating doses of curcumin (5, 10, 20, 25 μmol/L) or solvent only (DMSO) for different time periods (24, 48, 72 hours). All cell lines responded dose- and time-dependently to the curcumin exposition. The exponential growth of the tumor cells was abrogated completely after 24 hours using the second highest dose (20 μmol/L) in Tu-2449 and Tu-9648 cells, and with the highest dose (25 μmol/L) in Tu-251 cells.

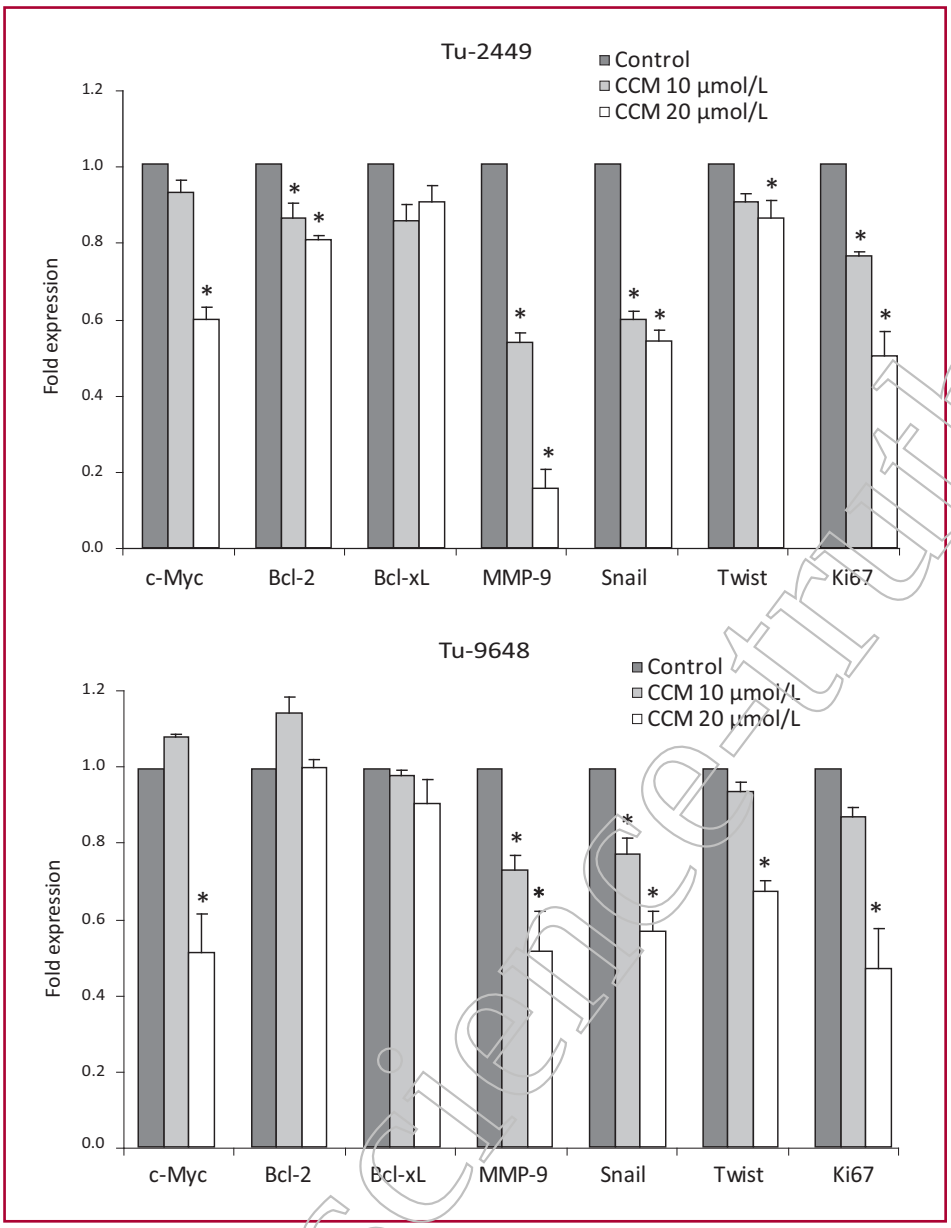

Fig. 2. Curcumin modulates STAT3 target gene expression in Tu-2449 and Tu-9648 cells. Cells were treated with solvent (Con) or 10 μmol/L and 20 μmol/L curcumin (CCM) for 24 hours. Total RNA was extracted and reverse transcribed. Transcripts of STAT3 target genes were quantified by real-time quantitative PCR using gene-specific TaqMan primers and probes. The Y-axis shows percentage fold changes in transcript expression normalized to control cultures. Bars, SD of triplicates; *, $P < 0.05$, significant difference between groups.

Curcumin induces G2/M phase arrest but not apoptosis

The activation of executioner caspases is a major hallmark of apoptotic cell death. To clarify whether growth retardation by curcumin was associated with apoptosis in Tu-2449, Tu-9648, and Tu-251 cells, we performed an *in vitro* assay, in which DEVD-AMC, a fluorogenic caspase 3 substrate was used to measure caspase 3-like activity. None of the cell lines showed a statistically significant increase in caspase 3-like activity, 24 hours following curcumin treatment (Fig. 3B). In line with this finding *in vitro*, none of the investigated tumor sections of curcumin-fed animals stained positive for activated caspase 3 or TUNEL (data not shown).

To further characterize the underlying mechanisms of the growth inhibitory effect of curcumin in murine glioma cells, we performed cell cycle analysis in Tu-2449, Tu-9648, and Tu-251 cells. Unsynchronized cells were exposed to escalating doses of curcumin (5, 10, 20 μmol/L) and incubated for 48 hours. Harvested cells were subjected to FACS analysis, which used DNA content as a measure of progression through the cell cycle and cell death. DNA flow cytometric analysis revealed that 5 μmol/L to 20 μmol/L curcumin induced a dramatic G2/M phase arrest in glioma cells following a 48 hours exposure (Fig. 3C), whereas the percentage of cells with sub-G1 DNA content was negligible. Collectively, these data suggest that the predominant growth inhibitory mechanism of curcumin in the examined cells was not induction of apoptosis but rather a G2/M arrest.

Curcumin impedes the migratory and invasive potential of murine glioma cells

Tu-2449 and Tu-9648 are glioma cell lines displaying highly invasive growth characteristics *in vivo* (23). In line with this, a strong correlation between STAT3 activity and the metastatic properties of other types of tumor cells is often observed (31). To test the effects of curcumin treatment on cell migration *in vitro*, a wound-healing assay was used, in which a scratch was created and Tu-2449, Tu-9648, and Tu-251 glioma cells were allowed to migrate into the scratched area. The number of migrated cells was determined 16 hours after scratching. In control cells treated with solvent only, 250 cells (Tu-2449, Tu-9648) and 200 cells (Tu-251) had migrated in the denuded area. In comparison, treatment with escalating doses of curcumin (5, 10, 20 μmol/L) led to an incremental attenuation of migration, with approximately 20 migrated cells at the highest dose (20 μmol/L) compared with more than 200 in controls (Fig. 4A and B).

To determine whether curcumin also affects the invasive potential of the Tu-2449, Tu-9648, and Tu-251 glioma cells *in vitro*, a modified Boyden-chamber assay was employed. Again, all cell lines showed a dose-dependent decrease of invaded cells with maximum effects at the highest dose (20 μmol/L), whereas DMSO used as control allowed up to 5-fold more cells to transmigrate the matrigel-coated pores (Fig. 4C and D). The observed changes were not because of alterations in cell viability (Fig. 3).

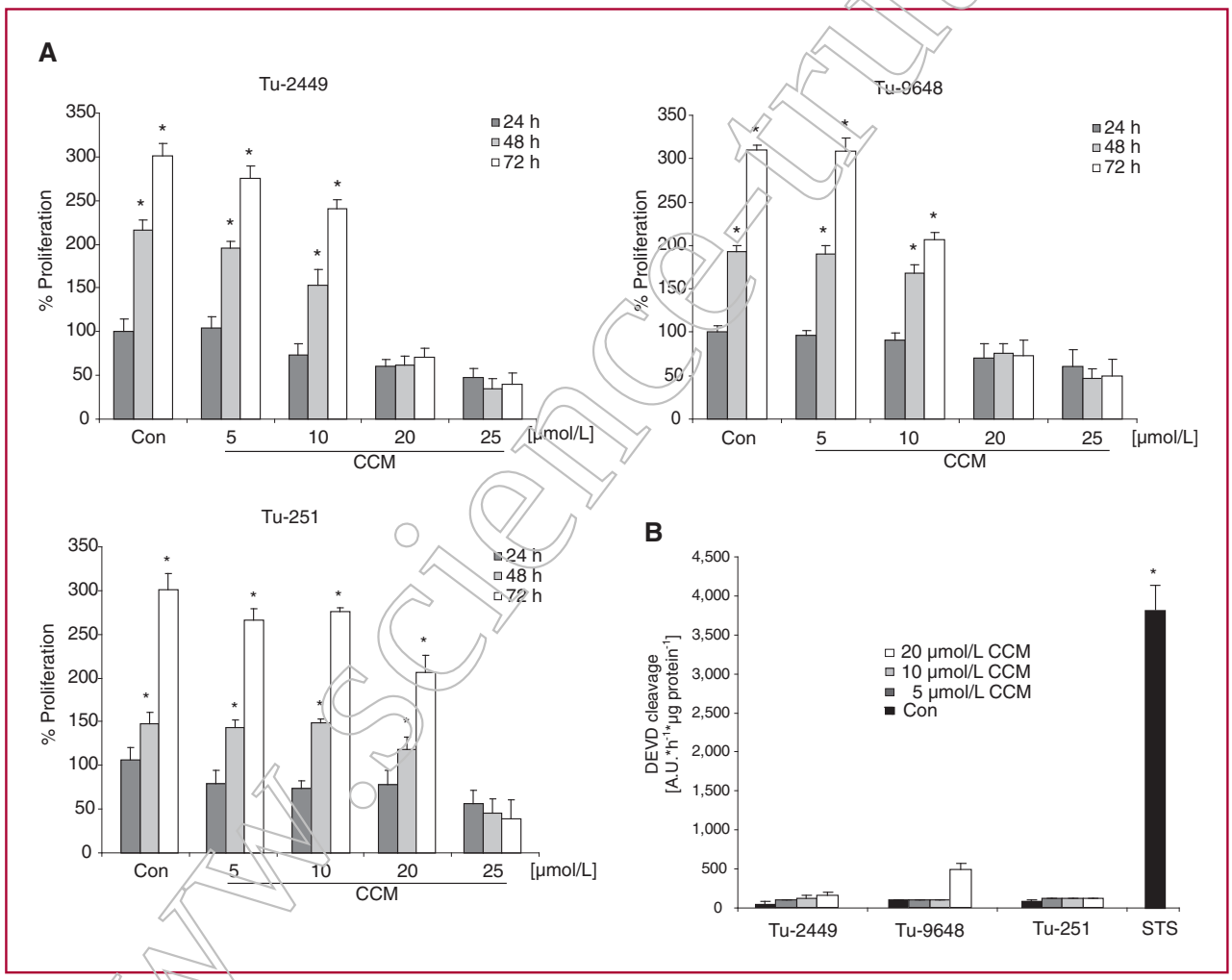

Fig. 3. Curcumin suppresses proliferation of Tu-2449, Tu-9648, and Tu-251 cells. A, cells were plated and grown for 24 hours and then treated with solvent only (Con) or escalating doses of curcumin (CCM) as indicated and harvested after 24 (dark), 48 (middle), and 72 (bright) hours. Cell viability was examined by using the MTT assay. The Y-axis shows percentage changes in absorbance at 570 nm; bars, SD of triplicates: *, $P < 0.05$, significant difference between groups. B, curcumin does not induce apoptosis in Tu-2449, Tu-9648, and Tu-251 cells. Cells were treated with escalating doses of curcumin (CCM) as indicated for 24 hours and subsequently examined for induction of apoptotic cell death by a caspase-3-like activity assay. As a positive control, cells were treated with staurosporin (STS) at a concentration of 3 μmol/L for 6 hours. Data are mean ± SEM from $n = 4$ independent cultures. *, $P < 0.05$, significant difference compared with the control (DMSO).

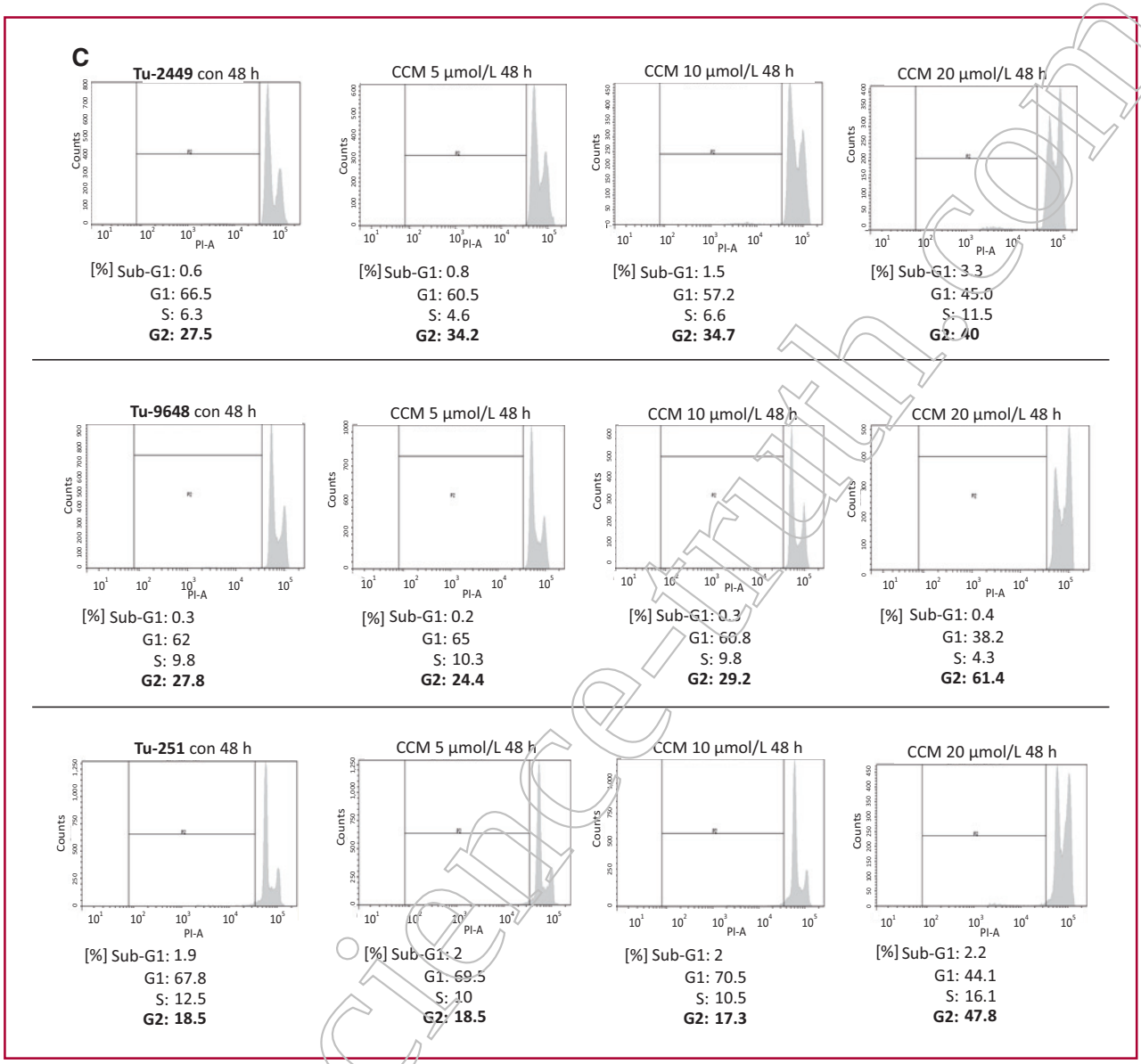

Fig. 3. *(Continued)*. C, curcumin induces a G2/M cell-cycle arrest in murine glioma cells. DNA flow cytometric analysis of Tu-2449, Tu-9648, and Tu-251 cells treated with indicated escalating doses of curcumin (CCM) for 48 hours. Histograms and cell cycle distributions shown are representative of 3 independent experiments.

Enforced expression of STAT3C rescues glioma cells from the curcumin-mediated effects

To further clarify whether the ability of curcumin to impede the migratory and invasive potential of murine glioma cells was caused by inhibition of STAT3, we examined whether a constitutively dimerized and thus persistently activated STAT3 could rescue glioma cells from the inhibitory effects of curcumin. To this end we transiently transfected Tu-2449 and Tu-9648 cells with a mutant form of STAT3 (STAT3C) that is active without tyrosine phosphorylation (15). In comparison to mock-transfected control cells, glioma cells transfected with STAT3C and treated with 10 and 20 μmol/L curcumin showed a significant increase in invasion (Fig. 5A). Similarly, the curcumin-mediated dose-dependent reduction in migration could be rescued by transiently overexpressing STAT3C (Fig. 5B). Transient expression of STAT3C in Tu-2449 and Tu-9648 cells was confirmed by Western blot analysis showing increased STAT3 protein levels in STAT3C-transfected cells compared with mock-transfected controls (Fig. 5C). The increase in sequence-specific DNA binding of active STAT3 in the mock- and STAT3C-transfected cell was determined by an ELISA-based method (Fig. 5D and E). Taken together, these rescue experiments imply that inhibition of STAT3's transcriptional activity in murine glioma cells plays an important role for the observed curcumin-mediated antiglioma effects.

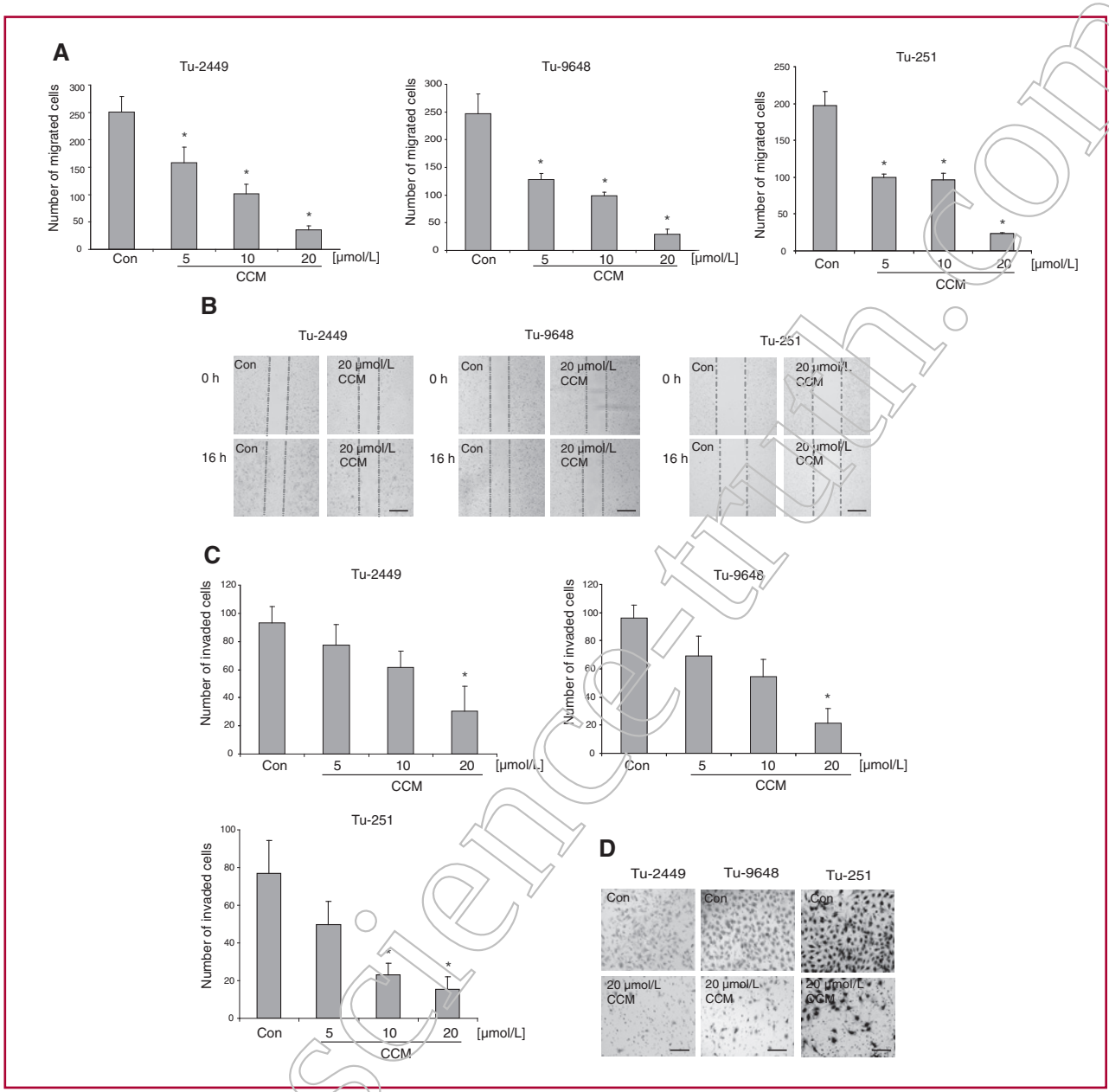

Fig. 4. Curcumin attenuates migration and invasion of Tu-2449, Tu-9648, and Tu-251 glioma cells. A, migration was analyzed using the wound healing assay. A single scratch was made in the confluent monolayer. The scratch was photographed at 0 hour and after 16 hours treatment with solvent (Con) or with the indicated increasing doses of curcumin. Cells that had migrated into the scratch were counted. The data represent 3 independent experiments. Bars, SD of triplicates; *, $P < 0.05$, significant difference between groups. B, representative photographs of scratch assays. Scale bar = 250 μm. C, invasiveness of Tu-2449, Tu-9648, and Tu-251 cells was examined using the ECM-coated Boyden-chamber assay. Cells were plated in the upper chamber of the transwell insert and incubated with increasing doses of curcumin as indicated. After 24 hours, cells were fixed to the membrane and stained to determine the number of invaded cells. The assay was done in triplicates. Bars, SD of triplicates; *, $P < 0.05$, significant difference between groups. D, representative photographs of transwell assays. Scale bar = 1 mm.

Curcumin intake effects tumor-free survival in immunocompetent animals bearing intracranial tumors

Because curcumin when injected into the tail vein can reach the brain and suppress melanoma growth in the brain (32), we here set out to assess whether dietary administered curcumin could counteract glioma tumor growth in an immunocompetent mouse model of glioma. To this end syngeneic B6C3F1 recipients were fed a Western-type diet, enriched in fat and cholesterol that was fortified with curcumin or not. Laboratory investigations suggested that a high-fat diet is associated with increased

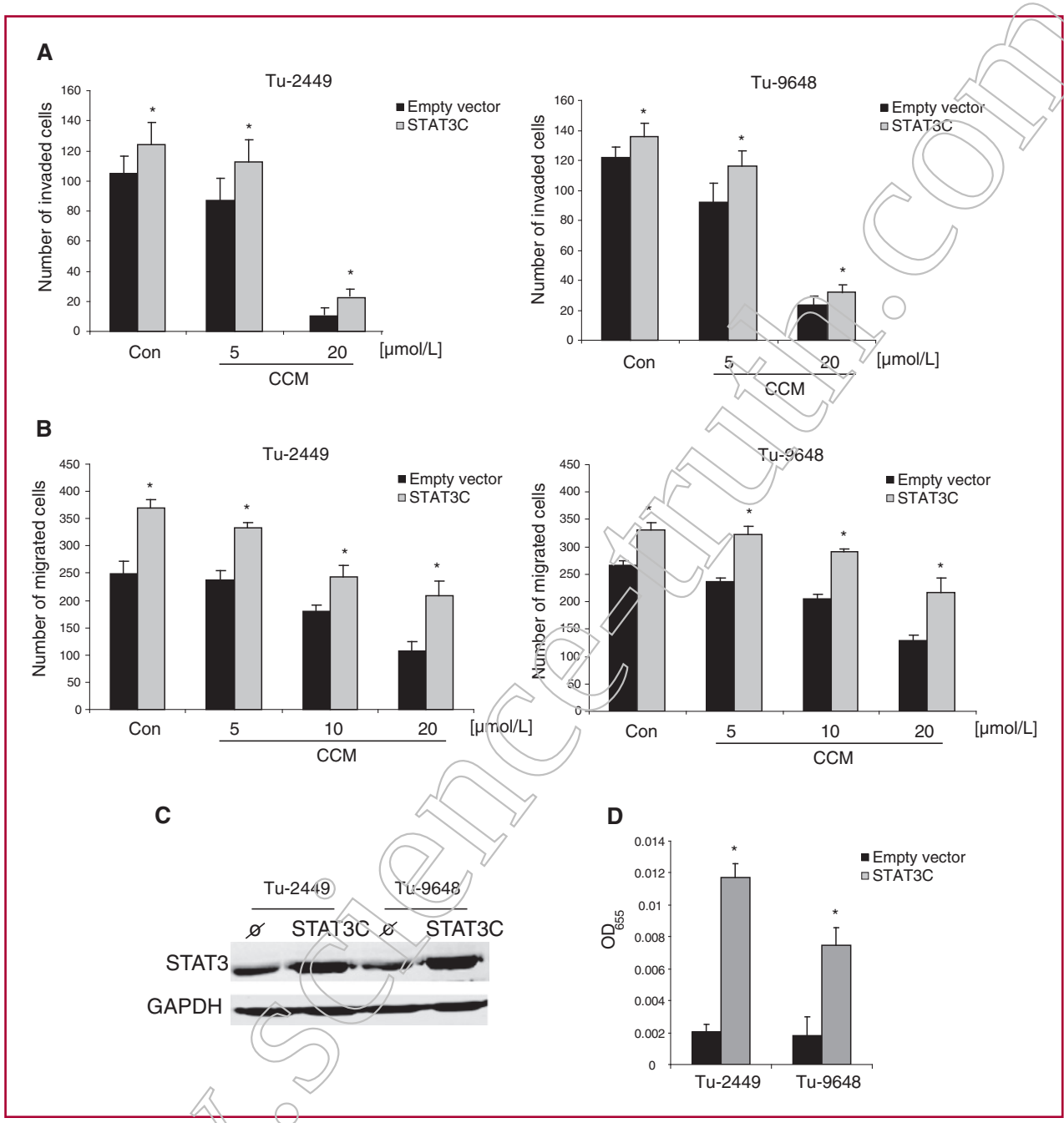

Fig. 5. Constitutively dimerized and active STAT3C rescues cells from curcumin-mediated effects. A, mock- (empty vector) and STAT3C-transfected (STAT3C) Tu-2449 and Tu-9648 cells were treated with solvent (Con) or escalating doses of curcumin (CCM) as indicated and assayed in the Boyden chamber for their invasiveness as described earlier in the text. The assay was done in triplicates. Bars, SD of triplicates; *, $P < 0.05$, significant difference between groups. B, in a similar fashion mock-transfected (empty vector) and STAT3C-transfected (STAT3C) were assayed for their migratory potential in wound healing assays. The data represent 3 independent experiments. Bars, SD of triplicates; *, $P < 0.05$, significant difference between groups. C, Western blot analysis of transiently mock- and STAT3C-transfected Tu-2449 and Tu-9648 cells harvested after 48 hours using a using a pan-STAT3 antibody (STAT3α). D, DNA-binding assay for active STAT3. Samples of mock- and STAT3C-transfected Tu-2449 and Tu-9648 cells harvested after 48 hours were applied to the wells and formed DNA transcription factor complexes were detected with an STAT3-specific antibody and then measured with the help of a colorimetric reaction reminiscent of an ELISA.

susceptibility to cancer (33, 34). The mice were pre-fed for 7 days with control or experimental diet and then implanted intracranially with either Tu-2449 or Tu-9648 glioma cells and kept on the respective diet over the whole observation period of 65 and 80 days, respectively. Brains were harvested when mice showed clinical symptoms or at the end of the observation period. Of the 2 glioma cell lines employed, Tu-2449 was more aggressive with a time to

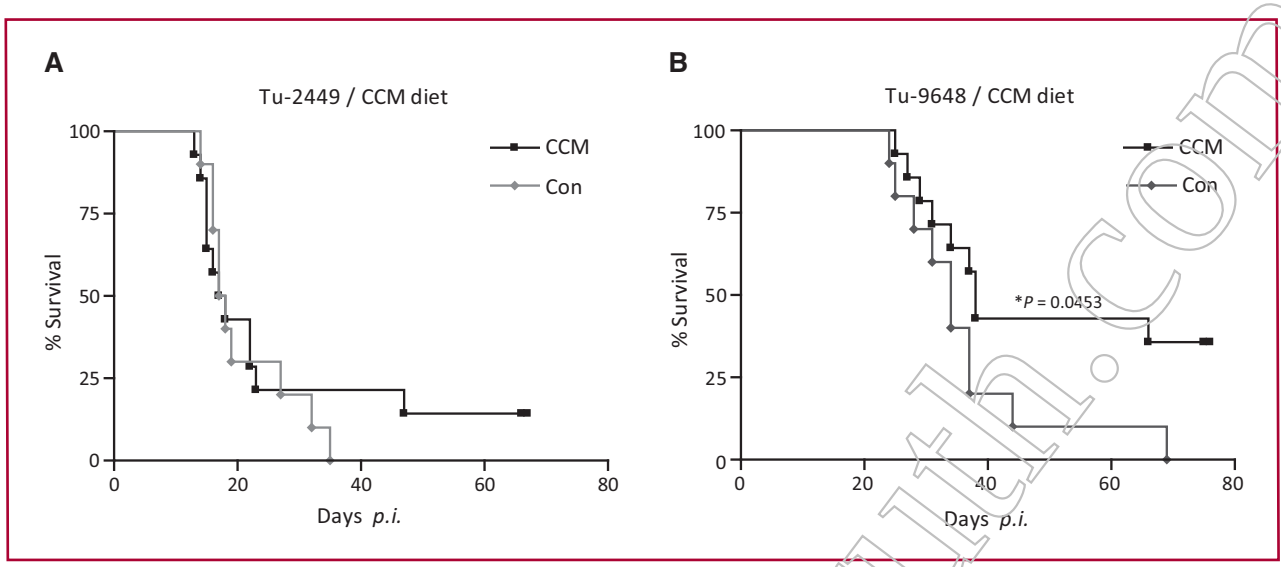

Fig. 6. Curcumin (CCM) entails tumor-free survival in mice bearing intracranial gliomas. Kaplan–Meier survival curves of animals from the different treatment groups ($n = 15$). A, in Tu-2449–bearing mice, curcumin treatment resulted in 15% tumor-free long-term survival, whereas all control animals died. B, in Tu-9648-bearing mice curcumin treatment resulted in 38% tumor-free long-term survival ($^*P < 0.05$), whereas all control animals died. (p.i., post implantation)

tumor onset of 14 days postimplantation compared with Tu-9648 with 35 days. In addition, the time window, in which tumor-bearing animals became symptomatic, was narrower for Tu-2449 (14–35 days) than for Tu-9648 (35–69 days). In Tu-2449-bearing mice the survival curves were not significantly different ($P = 0.6272$) between control and treatment group with a median survival time of 17.5 days for both groups. However, in the group treated with curcumin, 15% of the animals experienced long-term survival exceeding 65 days, whereas in the control group all had deceased within 35 days (Fig. 6A). Histopathologic analysis of the mouse brains revealed that all long-term survivors were tumor-free. In Tu-9648-bearing mice the difference in overall survival was statistically significant ($^*P < 0.0453$) with a median survival time of 38 days for the control and 34 days for the curcumin group. Here, the curcumin-fortified diet produced a 38% increase in long-term survival versus the control diet, in which all but 1 (69 days) succumbed to the cancer before 44 days (Fig. 6B). Again, the long-term survivors in the treatment group failed to develop brain tumors even after 80 days.

Inhibition of STAT3 signaling by dietary curcumin is associated with reduced tumor size, cell proliferation, and midline crossing in intracranial tumors

Figure 7A shows representative examples of coronal brain sections of a Tu-9648 tumor in comparison to tumor-free brain tissue, indicating that the tumor margin is not well circumscribed and that single tumor cells infiltrate the surrounding brain parenchyma. Only the glioma cells, particularly at the tumor margin and in the infiltration zone, stained positive for pY-STAT3 and Ki67 (Fig. 7A). Furthermore, immunohistochemical analysis with antibodies against GFAP revealed a reactive astrocytosis in the brain tissue adjacent to the glioma but not in tumor-free brains (Fig. 7A).

Because our experimental data *in vitro* suggested that inhibition of JAK1,2/STAT3 signaling by curcumin has led to reduced proliferation of glioma cells, we further scrutinized how curcumin would affect tumor growth *in vivo*. The efficacy of STAT3 inhibition by curcumin was assessed immunohistochemically comparing cells that stained positively for nuclear pY-STAT3 in treated and untreated tumor tissues. Figure 7B reflects the trend of dietary curcumin in reducing the numbers of cells with active, tyrosine-phosphorylated STAT3 in both intracranially implanted tumor cell lines, although the degree of reduction is statistically not significant. Morphometric analysis and immunohistochemical analysis with antibodies against the proliferation marker Ki67 revealed that both tumor size and tumor cell proliferation was reduced by curcumin in mice implanted with Tu-9648 cells (Supplementary Table S1). In mice implanted with Tu-2449 cells, there was a tendency toward decreased tumor size and proliferation of tumor cells. Moreover, midline crossing, that is, migration of intracranially implanted cells to the contra-lateral side was significantly diminished ($^{**}, P < 0.0051$) after curcumin treatment (Supplementary Table S1) in Tu-9648 tumors.

Discussion

Effective therapies for glioblastomas are scarce, and long-term survival is a rarity (35–37). Therefore, any new modality to replace or support current treatments for malignant gliomas would be helpful.

In this study, we evaluated the inhibitory effect of curcumin on malignant glioma cells. Our results show that

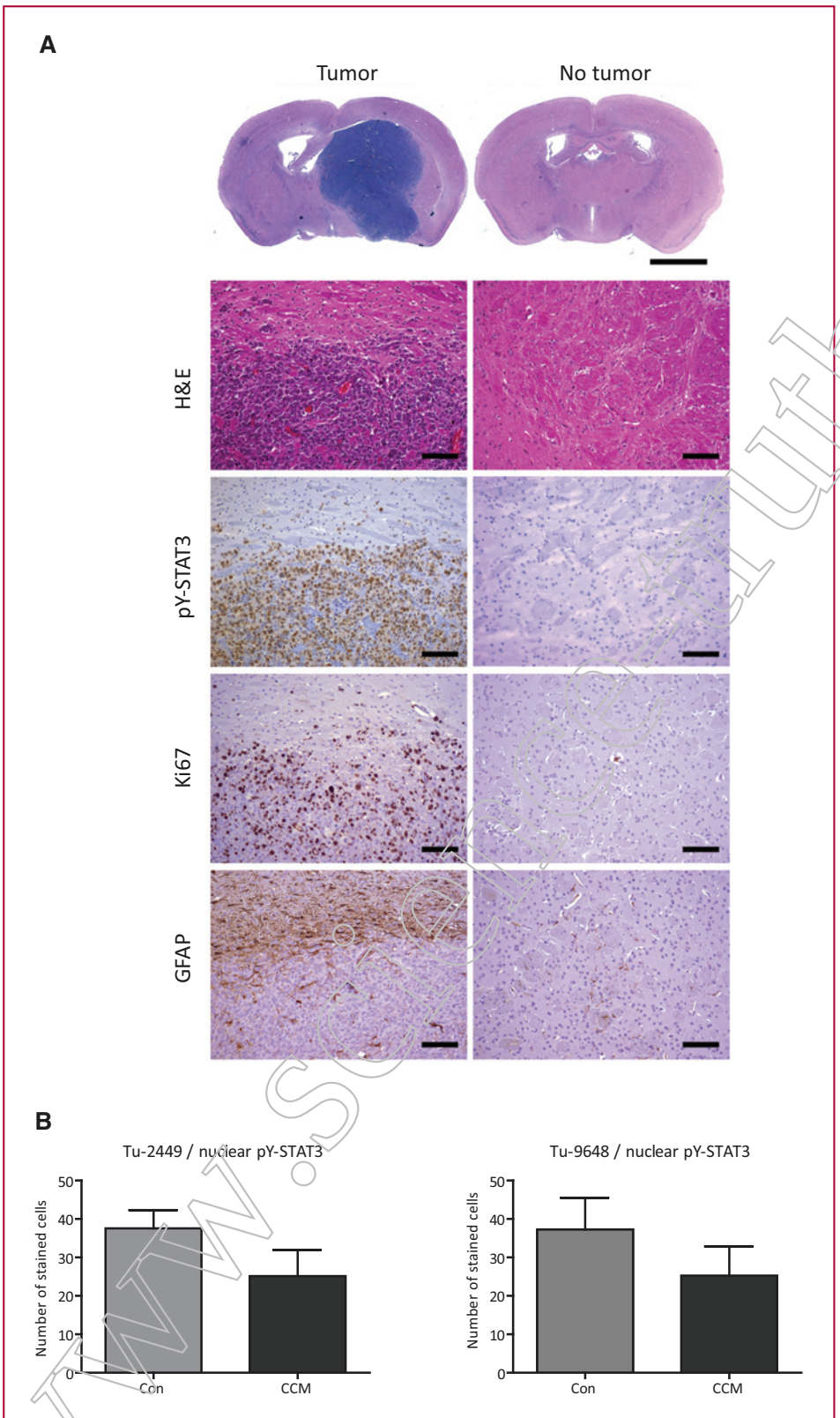

Fig. 7. Histologic and immunohistochemical characterization of mouse glioma and tumor-free tissue. A, top, a paraffin section of a mouse glioma is shown in hematoxylin & eosin (H&E) staining with a corresponding tumor-free mouse brain as control. Scale bar = 2 mm. Note the midline shift due to herniation of vast tumor mass invading from the left hemisphere. Bottom, the edge of the tumor and corresponding tissue in tumor-free mouse brains is shown at a higher magnification in H&E staining and after immunohistochemical staining with antibodies against tyrosine-phosphorylated STAT3 (pY-STAT3), Ki67, and glial fibrillary acidic protein (GFAP). Note the invasion of brain tissue by Ki67-positive tumor cells and the expression of pY-STAT3 in mouse glioma in comparison with tumor-free brain tissue. GFAP staining shows reactive gliosis in the brain tissue adjacent to the tumor. Scale bar = 100 μm. B, evaluation of pY-STAT3 inhibition in curcumin (CCM)-treated *versus* solvent-treated tumors on paraffin-embedded brain sections stained immunohistochemically for nuclear pY-STAT3. Data represent analysis of Tu-2449 ($n = 12$) and Tu-9648 ($n = 6$) tumors.

curcumin inhibits STAT3 activity, cell growth, cell cycle progression, and invasiveness of 3 different murine glioma cell lines. We further show that daily intake of curcumin inhibits tumor growth and produces significant tumor-free survival in immunocompetent mice with orthotopically implanted gliomas. These results suggest that inhibition of JAK/STAT3 signaling by the nutraceutical curcumin may be an effective therapeutic approach for the treatment of glioblastoma patients.

The transcription factor STAT3 was recently considered to be a master regulator in human glioma and essential for maintaining tumor initiating capacity and ability to invade the normal brain (38). Moreover, Birner et al. (39) demonstrated that STAT3 tyrosine phosphorylation correlates with survival in patients with GBM. Therefore, STAT3 appears to be an attractive target for pharmacologic intervention. Here, we show that the active form of STAT3 (pY-STAT3) is extensively expressed in murine glioma cells *in vitro* and *in vivo*. Strong pY-STAT3 expression was detectable almost exclusively in glioma cells, whereas in the normal brain parenchyma only few scattered endothelial cells stained positive for active STAT3. These findings indicate that pY-STAT3 is a strong and selective glial tumor marker.

There are several strategies to inhibit the STAT3 signaling pathway, for instance using small molecules, decoy oligos, siRNA (10), or peptide aptamers (40). However, formulations for clinical application and potential adverse side effects of these agents when applied in humans are not well studied. In contrast, curcumin is a popular dietary supplement that has been shown to have a wide variety of beneficial effects including antioxidant, anti-inflammatory, antiviral, antibacterial, antifungal, and anticancer activities, which are mediated through regulation of various transcription factors, inflammatory cytokines, protein kinases, and other enzymes (41). Several mechanisms by which curcumin exerts its anticancer effect have been reported, in the first line by inhibition of NF-κB (20). However, GBM cells were found to have little or no active NF-κB (42), and when in curcumin-treated GBM cells NF-κB p65 was knocked down, the viability of these cells did not change suggesting that the anticancer effect of curcumin seen in these cells was not caused by inhibition of NF-κB (7).

In this study, we found that the *in vitro* and *in vivo* antiglioma activity of curcumin can be attributed to downregulation of JAKs that are located upstream of STAT3 at gp130 where they convey external stimuli into the cell (30), presumably via activation of the tyrosine phosphatase SHP-2, a negative regulator of JAK activity (43). Curcumin inhibited STAT3 tyrosine phosphorylation much faster (2 hours) and at lower doses (20 μmol/L) when compared with the STAT3 inhibitory effect of another JAK2 inhibitor AG490 (48 hours; 100 mmol/L) in human GBM cells (26). We further found that STAT3 inhibition was paralleled by reduced cell growth *in vitro* and *in vivo* as monitored by MTT reduction assay and Ki67 labeling, respectively. In addition, we found by DNA flow cytometric analysis that curcumin induced an accumulation of glioma cells in the G2/M phase of the cell cycle. Because STAT3 was shown to control the expression of G2/M regulators in intestinal epithelial cells (44), the induced phase arrest in G2/M after curcumin-mediated STAT3 inhibition might be the underlying mechanism for the observed growth inhibition in murine gliomas.

The efficacy of curcumin to suppress STAT3 activity was also exemplified by the reduced immunoreactivity for pY-STAT3 selectively in glioma cells of intracranially implanted tumors compared with controls. In the investigated glioma cell lines, we could show by real-time RT-PCR that curcumin specifically downregulated the expression of protumorigenic STAT3 target genes having prosurvival activity such as c-Myc (15), or being implicated in epithelial-mesenchymal transition such as Snail and Twist (45), and being crucial for invasion and tumor cell dissemination such as extracelluar matrix degrading enzymes MMP-2 and MMP-9 (31).

The limited success of current treatment regimens (35, 46) is mainly caused by the ability of malignant glioma cells to diffusely infiltrate the surrounding healthy brain, a hallmark of glioblastoma that is recapitulated in our syngeneic mouse model of glioma (23). Characteristic migratory patterns include spread along white matter tracts (46). *In vivo*, curcumin reduced the midline crossing of glioma cells in Tu-9648 tumors in a highly significant ($^*P < 0.0051$) manner. Likewise, curcumin exposition *in vitro* significantly decreased invasiveness through matrigel-coated pores. Because curcumin potently suppressed STAT3 tyrosine phosphorylation rapidly and decreased transcription of MMP-2 and MMP-9 dietary curcumin might have also curbed infiltration *in vivo*.

We chose a Western-type diet enriched in fat and cholesterol for our study, because we felt that this would mimic eating habits of cancer patients. However, in B6C3F1 mice there were no obvious differences in time to tumor onset between feeding standard pellets and Western-type pellets (data not shown). Given that a recipient mouse weighed 20 g and ate 4 g mouse chow containing 500 mg/kg curcumin per day it might have ingested approximately 100 μg curcumin. Several phase I clinical trials have shown that curcumin was well tolerated up to 12 g per day without major adverse effects, and a dose of 8 g curcumin per day showed therapeutic efficacy in patients with colon cancer (47). Estimating that an average individual weighs 80 kg, a dose of 8 g per day in humans would equal the daily dose of 100 μg in mice applied in our study. The same dose given intraperitoneally to female mice yielded a peak plasma level of 2.25 mg/L (~6 μmol/L) 15 minutes after injection declining rapidly within 1 hour (48). Such a curcumin plasma concentration would be in the lower molar range used in *in vitro* experiments, nevertheless showing antiglioma effects.

An increasing number of studies have shown the anticancer efficacy of curcumin in various murine cancer

models (47). In our preclinical study we could demonstrate that curcumin has a chemopreventive activity against orthotopically implanted glioma in immunocompetent hosts. In nude mice xenotransplanted with glioma cells subcutaneously into the flanks, curcumin exerted its tumor-suppressive activity also in a therapeutic fashion, that is, after tumor establishment (49). *In vivo*, when given in the mouse chow, Kaplan–Meier survival plots showed a significant increase in the median survival in Tu-9648 and a modest one in Tu-2449 tumor-bearing mice, hinting to a more malignant genetic make-up. Nevertheless, curcumin feeding led in 2 different glioma cell lines to increased survival. The increase in survival is thought to be the result of curcumin's inhibitory capacity to attenuate the glioma cells' proliferative, migratory and invasive behavior seen *in vitro*.

Immune evasion is a major reason for tumor formation and tumor progression (16). Gene expression analysis of murine glioma cells grown *in vitro* versus intracranially in immunocompetent mice versus intracranially in athymic nude revealed that the respective tumors displayed unique signatures, and that the discriminating genes belonged to the immunomodulatory compartment (50). Tumor-secreted factors, such as IL-6, IL-10, and VEGF can activate STAT3 in dendritic cells, resulting in their impaired maturation, antigen-specific T-cell responses, and tumor evasion (16). On the other hand, knockdown of STAT3 in intracranial GL261 gliomas led to microglia and macrophage activation thus reversing immunosuppression and inhibiting tumor growth *in vivo* (51). In addition, systemic intraperitoneal administration of the STAT3 inhibitor JSI-124 resulted in long-term survival of GL261-bearing immunocompetent mice, but not of tumor-bearing athymic mice, suggesting a role of adaptive immunity in the observed antitumor effect (52). In intraperitoneally curcumin-treated immunocompromised mice (49), the survival time of treated animals was prolonged, yet did not prevent death. In contrast, the therapeutic effect of dietary curcumin in our immunocompetent mice occurred relatively late, but lead to a significant proportion of tumor-free long-term survivors, suggesting a potential involvement of adaptive immunity.

In summary, this is the first report demonstrating therapeutic effects of dietary curcumin on glioma growth in immunocompetent mice. Our results gained from 2 different malignant glioma cell lines confirmed the potential suitability of curcumin for chemopreventive applications in malignant brain tumors. Curcumin's safety makes it a good candidate for preventive or complementary therapy (47). Because curcumin shows poor systemic bioavailability after oral administration, experiments are planned to enhance the bioavailability of curcumin in the brain by using new formulations such as micronization and micellation or in combination with piperine (53).

Disclosure of Potential Conflicts of Interest

No potential conflicts of interest were disclosed.

Acknowledgments

We thank Christina Matreux for excellent technical assistance and Jan Frank for helpful discussions.

Grant Support

This study was funded by the German Research Foundation (WE 4358/1) and the LOEWE program (OSF) of the state of Hessia.

Received 02/24/2010; revised 07/09/2010; accepted 07/29/2010; published online 12/07/2010.

References

1. Ohgaki H, Kleihues P. Genetic pathways to primary and secondary glioblastoma. Am JPathol 2007;170:1445–53
2. Lesniak MS, Brem H. Targeted therapy for brain tumours. Nat Rev Drug Discov 2004;3:499–508.
3. Stupp R, Hegi ME, Gilbert MR, Chakravarti A. Chemoradiotherapy in malignant glioma: standard of care and future directions. J Clin Oncol 2007;25:4127–36.
4. Ryu MJ, Cho M, Song JY, Yun YS, Choi IW, Kim DE, et al. Natural derivatives of curcumin attenuate the Wnt/beta-catenin pathway through down-regulation of the transcriptional coactivator p300. Biochem Biophys Res Commun 2008;377:1304–8.
5. Luthra PM, Kumar R, Prakash A. Demethoxycurcumin induces Bcl-2 mediated G2/M arrest and apoptosis in human glioma U87 cells. Biochem Biophy Res Commun 2009;384:420–5.
6. Dhandapani KM, Mahesh VB, Brann DW. Curcumin suppresses growth and chemoresistance of human glioblastoma cells via AP-1 and NFkappaB transcription factorsJ Neurochem 2007;102:522–38.
7. Aoki H, Takada Y, Kondo S, Sawaya R, Aggarwal BB, Kondo Y. Evidence that curcumin suppresses the growth of malignant gliomas *in vitro* and *in vivo* through induction of autophagy: role of Akt and extracellular signal-regulated kinase signaling pathways. Mol Pharmacol 2007;72:29–39.
8. Kim SY, Jung SH, Kim HS. Curcumin is a potent broad spectrum inhibitor of matrix metalloproteinase gene expression in human astroglioma cells. Biochem Biophys Res Commun 2005;337:510–6.
9. Furnari FB, Fenton T, Bachoo RM, Mukasa A, Stommel JM, Stegh A, et al. Malignant astrocytic glioma: genetics, biology, and paths to treatment. Genes Dev 2007;21:2683–710.
10. Brantley EC, Benveniste EN. Signal transducer and activator of transcription-3: a molecular hub for signaling pathways in gliomas. Mol Cancer Res 2008;6:675–84.
11. Takeda K, Noguchi K, Shi W, Tanaka T, Matsumoto M, Yoshida N, et al. Targeted disruption of the mouse Stat3 gene leads to early embryonic lethality.Proc Natl Acad Sci U S A 1997;94:3801–4.
12. Akira S. Roles of STAT3 defined by tissue-specific gene targeting. Oncogene 2000;19:2607–11.
13. Sano S, Itami S, Takeda K, Tarutani M, Yamaguchi Y, Miura H, et al. Keratinocyte-specific ablation of Stat3 exhibits impaired skin remodeling, but does not affect skin morphogenesis. EMBO J 1999;18:4657–68.
14. Sano S, Chan KS, Carbajal S, Clifford J, Peavey M, Kiguchi K, et al. Stat3 links activated keratinocytes and immunocytes required for development of psoriasis in a novel transgenic mouse model. Nat Med 2005;11:43–9.

15. Bromberg JF, Wrzeszczynska MH, Devgan G, et al. Stat3 as an oncogene. Cell 1999;98:295–303.
16. Yu H, Pardoll D, Jove RSTATs in cancer inflammation and immunity: a leading role for STAT3. Nat Rev Cancer 2009;9:798–809.
17. Schlessinger K, Levy DE. Malignant transformation but not normal cell growth depends on signal transducer and activator of transcription 3. Cancer Res 2005;65:5828–34.
18. Weissenberger J, Loeffler S, Kappeler A, Kopf M, Lukes A, Afanasieva TA, et al. IL-6 is required for glioma development in a mouse model. Oncogene 2004;23: 3308–16.
19. Wang H, Lathia JD, Wu Q, Wang J, Li Z, Heddleston JM, et al. Targeting interleukin 6 signaling suppresses glioma stem cell survival and tumor growth. Stem Cells 2009;27:2393–404.
20. Bharti AC, Donato N, Aggarwal BB. Curcumin (diferuloylmethane) inhibits constitutive and IL-6-inducible STAT3 phosphorylation in human multiple myeloma cells. J Immunol 2003; 171;3863–71.
21. Konnikova L, Kotecki M, Kruger MM, Cochran BH. Knockdown of STAT3 expression by RNAi induces apoptosis in astrocytoma cells. BMC Cancer 2003;323.
22. Iwamaru A, Szymanski S, Iwado E, Aoki H, Yokoyama T, Fokt I, et al. A novel inhibitor of the STAT3 pathway induces apoptosis in malignant glioma cells both *in vitro* and *in vivo*. Oncogene 2007;26:2435–44.
23. Smilowitz HM, Weissenberger J, Weis J, Brown JD, O'Neill RJ, Laissue JA. Orthotopic transplantation of v-src-expressing glioma cell lines into immunocompetent mice: establishment of a new transplantable *in vivo* model for malignant glioma. J Neurosurg 2007; 106:652–9.
24. Weissenberger J, Steinbach JP, Malin G, Spada S, Rulicke T, Aguzzi A. Development and malignant progression of astrocytomas in GFAP-v-src transgenic mice. Oncogene 1997;14:2005–13.
25. Loeffler S, Fayard B, Weis J, Weissenberger J. Interleukin-6 induces transcriptional activation of vascular endothelial growth factor (VEGF) in astrocytes *in vivo* and regulates VEGF promoter activity in glioblastoma cells via direct interaction between STAT3 and Sp1. Int J Cancer 2005;115:202–13.
26. Senft C, Priester M, Polacin M, Schroder K, Seifert V, Kogel D, et al. Inhibition of the JAK-2/STAT3 signaling pathway impedes the migratory and invasive potential of human glioblastoma cells. J Neurooncol. [Epub ahead of print].
27. Voss V, Senft C, Lang V, Ronellenfitsch MW, Steinbach JP, Seifert V, et al. The Pan-Bcl-2 inhibitor (-)-Gossypol triggers autophagic cell death in malignant glioma. Mol Cancer Res. [Epub ahead of print].
28. Livak KJ, Schmittgen TD. Analysis of relative gene expression data using real-time quantitative PCR and the 2(-Delta Delta C(T)) Method. Methods 2001;25:402–8.
29. Hekmatara T, Bernreuther C, Khalansky AS, Theisen A, Weissenberger J, Matschke J, et al. Efficient systemic therapy of rat glioblastoma by nanoparticle-bound doxorubicin is due to antiangiogenic effects. Clin Neuropathol 2009;28: 153–64.
30. Heinrich PC, Behrmann I, Haan S, Hermanns HM, Muller-Newen G, Schaper F. Principles of interleukin (IL)-6-type cytokine signalling and its regulation. Biochem J 2003;374:1–20.
31. Huang S. Regulation of metastases by signal transducer and activator of transcription 3 signaling pathway: clinical implications. Clin Cancer Res 2007;13:1362–6.
32. Purkayastha S, Berliner A, Fernando SS, Ranasinghe B, Ray I, Tariq H, et al. Curcumin blocks brain tumor formation. Brain Res [Epub ahead of print].
33. Yang W, Bancroft L, Nicholas C, Lozonschi I, Augenlicht LH. Targeted inactivation of p27kip1 is sufficient for large and small intestinal tumorigenesis in the mouse, which can be augmented by a Western-style high-risk diet. Cancer Res 2003;63:4990–6.
34. Singh J, Hamid R, Reddy BS. Dietary fat and colon cancer: modulating effect of types and amount of dietary fat on ras-p21 function during promotion and progression stages of colon cancer. Cancer Res 1997;57:253–8.
35. Holland EC. Glioblastoma multiforme: the terminator. Proc Natl Acad Sci USA 2000;97:6242–4.
36. McLendon RE, Halperin EC. Is the long-term survival of patients with intracranial glioblastoma multiforme overstated?Cancer 2003;98: 1745–8.
37. Bahr O, Herrlinger U, Weller M, Steinbach JP. Very late relapses in glioblastoma long-term survivors. J Neurol 2009;256:1756–8.
38. Carro MS, Lim WK, Alvarez MJ, Bollo RJ, Zhao X, Snyder EY, et al. The transcriptional network for mesenchymal transformation of brain tumours. Nature 2010;463: 318–25.
39. Birner P, Toumangelova-Uzeir K, Natchev S, Guentchev M. STAT3 tyrosine phosphorylation influences survival in glioblastoma. J Neurooncol. [Epub ahead of print]
40. Borghouts C, Kunz C, Delis N, Groner B. Monomeric recombinant peptide aptamers are required for efficient intracellular uptake and target inhibition. Mol Cancer Res 2008;6:267–81.
41. Aggarwal BB, Sundaram C, Malani N, Ichikawa H. Curcumin: the Indian solid gold. Adv Exp Med Biol 2007;595:1–75.
42. La Ferla-Bruhl K, Westhoff MA, Karl S, Kasperczyk H, Zwacka RM, Debatin KM, et al. NF-kappaB-independent sensitization of glioblastoma cells for TRAIL-induced apoptosis by proteasome inhibition. Oncogene 2007;26: 571–82.
43. Kim HY, Park EJ, Joe EH, Jou I. Curcumin suppresses Janus kinase-STAT inflammatory signaling through activation of Src homology 2 domain-containing tyrosine phosphatase 2 in brain microglia. J Immunol 2003;171:6072–9.
44. Bollrath J, Phesse TJ, von Burstin VA, Putoczki T, Bennecke M, Bateman T, et al. gp130-mediated Stat3 activation in enterocytes regulates cell survival and cell-cycle progression during colitis-associated tumorigenesis. Cancer cell 2009; 15:91–102.
45. Sullivan NJ, Sasser AK, Axel AE, Vesuna F, Raman V, Ramirez N, et al. Interleukin-6 induces an epithelial-mesenchymal transition phenotype in human breast cancer cells. Oncogene 2009;28:2940–7.
46. Claes A, Idema AJ, Wesseling P. Diffuse glioma growth: a guerilla war. Acta Neuropathol 2007;114:443–58.
47. Sharma RA, Gescher AJ, Steward WP. Curcumin: the story so far. Eur J Cancer 2005;41:1955–68.
48. Pan MH, Huang TM, Lin JK. Biotransformation of curcumin through reduction and glucuronidation in mice. Drug Metab Dispos 1999;27:486–94.
49. Perry MC, Demeule M, Regina A, Moumdjian R, Beliveau R. Curcumin inhibits tumor growth and angiogenesis in glioblastoma xenografts. Mol Nutr Food Res 2010;54:1192—201.
50. Learn CA, Grossi PM, Schmittling RJ, Xie W, Mitchell DA, Karikari I, et al. Genetic analysis of intracranial tumors in a murine model of glioma demonstrate a shift in gene expression in response to host immunity. J Neuroimmunol 2007;182:63–72.
51. Zhang L, Alizadeh D, Van Handel M, Kortylewski M, Yu H, Badie B. Stat3 inhibition activates tumor macrophages and abrogates glioma growth in mice. Glia 2009;57:1458–67.
52. Fujita M, Zhu X, Sasaki K, Ueda R, Low KL, Pollack IF, et al. Inhibition of STAT3 promotes the efficacy of adoptive transfer therapy using type-1 CTLs by modulation of the immunological microenvironment in a murine intracranial glioma.J Immunol 2008;180:2089–98.
53. Antony B, Merina B, Iyer VS, Judy N, Lennertz K, Joyal S. A Pilot cross-over study to evaluate human oral bioavailability of BCM-95CG (Biocurcumax), a novel bioenhanced preparation of curcumin. Indian J Pharm Sci 2008;70:445–9.

AACR American Association for Cancer Research

Clinical Cancer Research

Dietary Curcumin Attenuates Glioma Growth in a Syngeneic Mouse Model by Inhibition of the JAK1,2/STAT3 Signaling Pathway

Jakob Weissenberger, Maike Priester, Christian Bernreuther, et al.

Clin Cancer Res 2010;16:5781-5795.